Experimental study of flashing LNG jet fires following horizontal releases

Zhang Qian-xi[a,b] , Liang Dong [b,1], Jennifer.Wen [c,2]

[a] *College of Mechanical and Power Engineering, Guangdong Ocean University, Zhanjiang 524088, China*

[b]*Guangdong Provincial Key Laboratory of Fire Science and Technology, School of Engineering, Sun Yat-sen University, Guangzhou 510006, China*

[c]*Warwick FIRE, School of Engineering, Coventry CV4 7AL, United Kingdom*

ABSTRACT

A horizontally oriented jet fire could occur if the leaking liquefied natural gas (LNG) from the side surface of a pipe or storage tank was ignited. Previous work with LNG mostly focused on pool fires. In the present study, horizontally oriented LNG jet fires were studied through 10 open field full scale tests. The flames were visualized by both infrared and video cameras. The recorded flame shapes are compared and analysed. Peak temperatures and heat fluxes at various flow rates were measured and recorded. For relatively low reservoir pressure, a small amount of LNG was found to spray through the fire and rainout onto the ground, forming an LNG pool. A correlation was established to calculate the flame length from the mass flow rate.

Keywords: Flashing LNG jet fires; Field tests; Rain out, Fire characteristics; Incident radiative heat fluxes.

1. Introduction

There has been rapid increase in the use of natural gas (NG) due to the international commitment to reduce greenhouse gases emissions in recent years. It is anticipated that such trend will continue as NG is seen as a vital ally in the search for a sustainable energy future. Along with this trend, increasing number of NG is being transported in the form of liquefied natural gas (LNG) from the Middle East, Africa, USA and the Caribbean where there are large gas reserves via sea to other countries where NG supply is insufficient, e.g. Europe and China. Possessing the capacity to produce a considerable amount of gas (a ratio of ≈ 600:1 at standard

[1] gzliangd@163.com

[2] Jennifer.wen@warwick.ac.uk

temperature and pressure), LNG has made itself an enormously important constituent of the NG industry requiring high safety standards in storage, handling, and transportation. The failure of the insulation layer of LNG tanks or rupture of LNG pipelines could result in the leakage of LNG, and subsequently potential ignition. From the perspective of energy security and reliability, this has brought about a renewed focus on the safety of LNG.

The "boiling point" of LNG is -162°C. Upon releasing into the air, the LNG jet quickly evaporates and yields large volumes of LNG vapour. Ignition of the flashing LNG jet can result in large jet fires, posing hazards to nearby facilities and personnel. Using NG or a mixture of NG and hydrogen, Lowesmith and Hankinson (2012) carried out a series of horizontal large-scale jet fire experiments, which involved a 150mm diameter pipe that ruptured under the pressure of 70 bar. After the released gas was ignited in these experiments, a jet flame formed immediately, rose upwards rapidly until it burnt out. The length of the jet flame continued to increase, reached a maximum of about 100 meters, and then steadily shortened as the pipe depressurised. Palacios and Casal (2011) tested vertical propane jet fires and reported measurements of the flame shape, length and width. All these large-scale tests were conducted with gaseous fuels. According to the review of Raj (2007) and Cleaver et al. (2007), the previous tests for LNG fires included expanding pool fires on water and fixed size pool fires on land. To the best of the authors' knowledge, no tests of LNG jet fires have been reported in the public domain. As commented by Lowesmith et al. (2007), the pressurised release of a liquid can also give rise to a two-phase jet fire if the liquid is able to vaporise quickly. For pressurised release of LNG from containment to the ambient, flash evaporation occurs, the ignition of the flashing LNG jets can result in flashing LNG jet fires. For hazards assessment of LNG installation or facilities, it is important to have insight of the flame characteristics of the resulting jet fires and their thermal radiation hazards. Such knowledge will be essential to aid the development of mitigation and protection measures.

In the present study, full-scale tests were conducted with flashing LNG jet fires squirted from an adiabatic tube into still air at atmospheric pressure and temperature. The shape, length and temperature of the jet fires were analysed for tests with different mass flow rates. In addition, a mathematical expression for calculating the length of the jet fire was proposed.

2. Experimental setup and summary of the tests conducted

The jet fire tests were conducted in an open field at Guangzhou Fire Training Centre (GFTC) in Guangzhou, China. Figure 1 provides a schematic of the experimental setup. The measurements were conducted with 17 thermocouples, 5 radiometers, 1 heat flow meter, a normal CCD camera and an infrared camera. The K-type thermocouples were located at different locations along the jet direction as shown in Fig. 1.

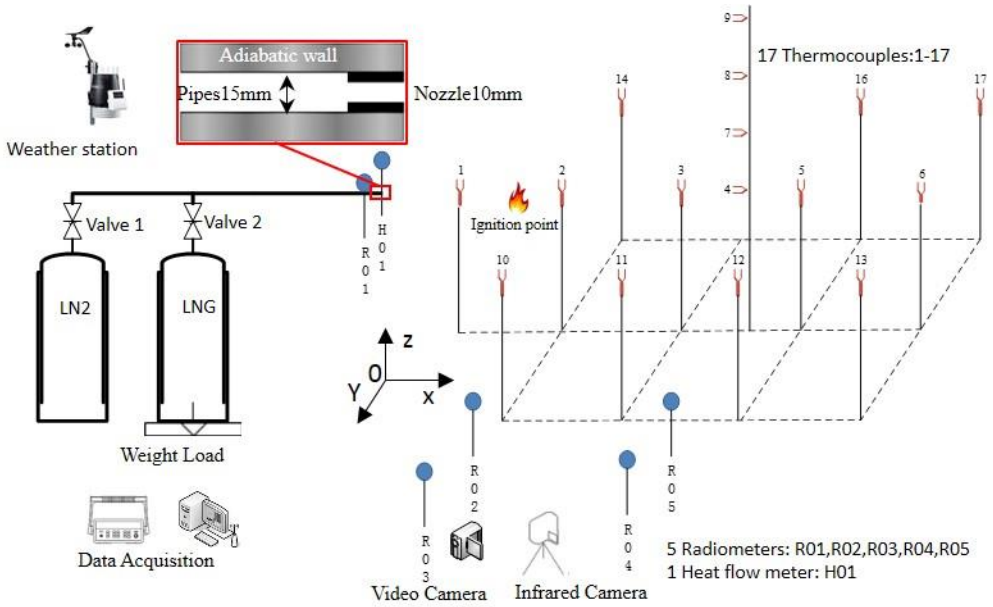

Fig. 1. Schematic diagram of the experimental system.

The temperature of the LNG was measured with T-type thermocouples situated at the right-hand side of the nozzle. Thermal radiation was measured by 5 radiometers of three ranges (Gardon gauge type, Medtherm Corporation, USA): 50 kW/m^2, 100 kW/m^2 and 200 kW/m^2. The radiometers were installed at a height of 1.5 m above the ground. A heat flow meter was used to monitor the heat transferred to the nozzle from the jet fire. An LNG Dewar tank was placed on a load cell to measure its weight throughout the blowdown process. The internal pressure was also monitored using a pressure gauge with a pressure range between 0 ~ 27.58 bar. Both an ordinary CCD camera and an infrared camera FLIR T660 were used to record the flame images. The later possesses such functions as recording images of 640×480 pixels and detecting black body temperatures up to two thousand centigrade. A meteorological weather station measured the ambient temperature, wind speed and direction, relative humidity and solar radiation. Agilent 34970A hardware was used for data acquisition. Pre-test preparations were carried out by employing liquid nitrogen (LN_2) to cool down the connecting pipes and check for any leakage at the connecting valves. The precision of the instruments is shown in Table 1.

Table 1 The precision of the instruments

Instruments	**Precision**
K-type thermocouples	±（1%rdg+1℃）
T-type thermocouples	±1℃
Radiometers	±3%
Heat flow meter	±3%
Infrared camera FLIR T660	±2℃
Electronic balance	±4g

The LNG used in the experiment was provided by a gas station in Dongguan, Guangdong. Its compositions are shown in Table 2. The LNG Dewar tank has a self-pressurized regulating valve that ensured the LNG to be released under certain pressure. The release rate of the LNG was measured by an electronic balance at the bottom of the tanker as described above.

Table 2 Composition of the LNG

Ingredients	**Mole fraction**	
Carbon Dioxide	2.529	mol%
Nitrogen	0.146	mol%
Methane	91.654	mol%
Ethane	5.423	mol%
Propane	0.246	mol%
Iso-Butane	0.002	mol%
N-Butane	0.000	mol%
Iso-Pentane	0.000	mol%
N-Pentane	0.000	mol%
Hexanes Plus	0.000	mol%
TOTAL	100.000	mol%

Altogether 20 tests were conducted over two days with varied LNG flow rates, ranging between 0.01 and 0.075kg/s. The results from a series of ten horizontal releases are reported in the present manuscript. A summary of the test conditions is given in Table 3.

Table 3 Test conditions

Property	Value
Air temperature (°C)	29.3 ±3.6
Relative humidity (%)	70.9 ± 9.3
Wind speed (m/s)	0-0.05
Rain (mm)	0
Release diameter(mm)	10
Release pressure(bar)	5.2-10.1
Mass flow rate(kg/s)	0.01, 0.021, 0.04, 0.075

3. Results

3.1 The burning characteristics of the flashing LNG jet fires

Figure 2 is a snapshot of the released LNG jet before ignition. Following the release of the pressurised LNG, the flow was chocked at the orifice, resulting in an under-expanded sonic jet, which contained complex repeated shock structures. As the ambient temperature was much higher than the boiling point of LNG, which was approximately -162℃, flashing occurred immediately. This was followed by the atomisation of the liquid stream as the LNG expanded to atmospheric pressure and evaporated. The initial LNG jet was denser than the air due to the relatively low temperature. The low temperature of the LNG vapour also caused condensation of the moisture in the atmosphere. As a result, the LNG vapour appeared white. Following heat exchange with the surrounding air, its temperature gradually increased. This was accompanied by the gradual decrease of its density. The observations are consistent with previous experimental reports (Koopman et al., 1982; Puttock et al., 1982; Havens, 1992.

Fig. 2. The flashing LNG jet before ignition.

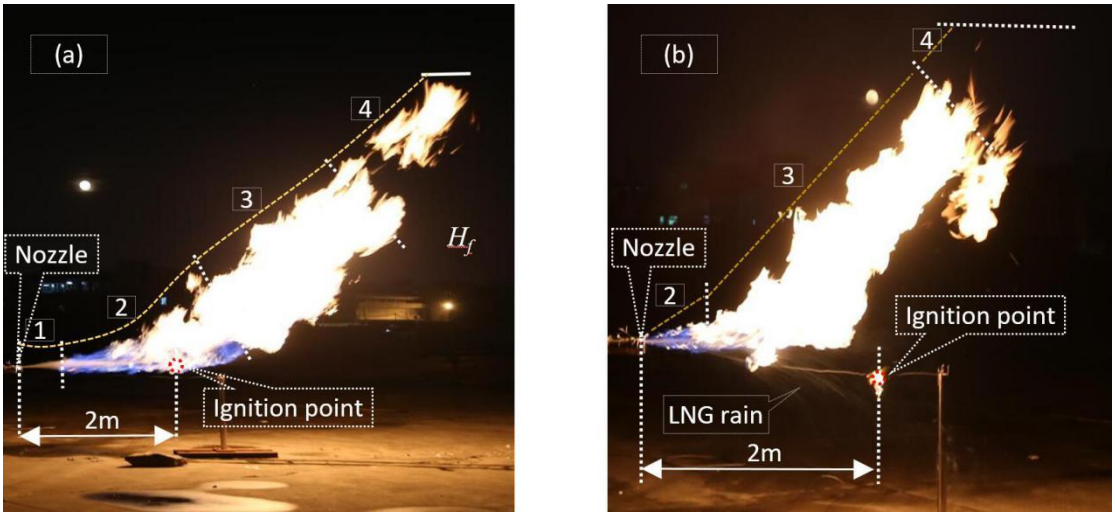

Fig.3. Snapshots of the ignited LNG jets: (a) LNG flow rate 0.04kg/s; (b) LNG flow rate 0.02kg/s.

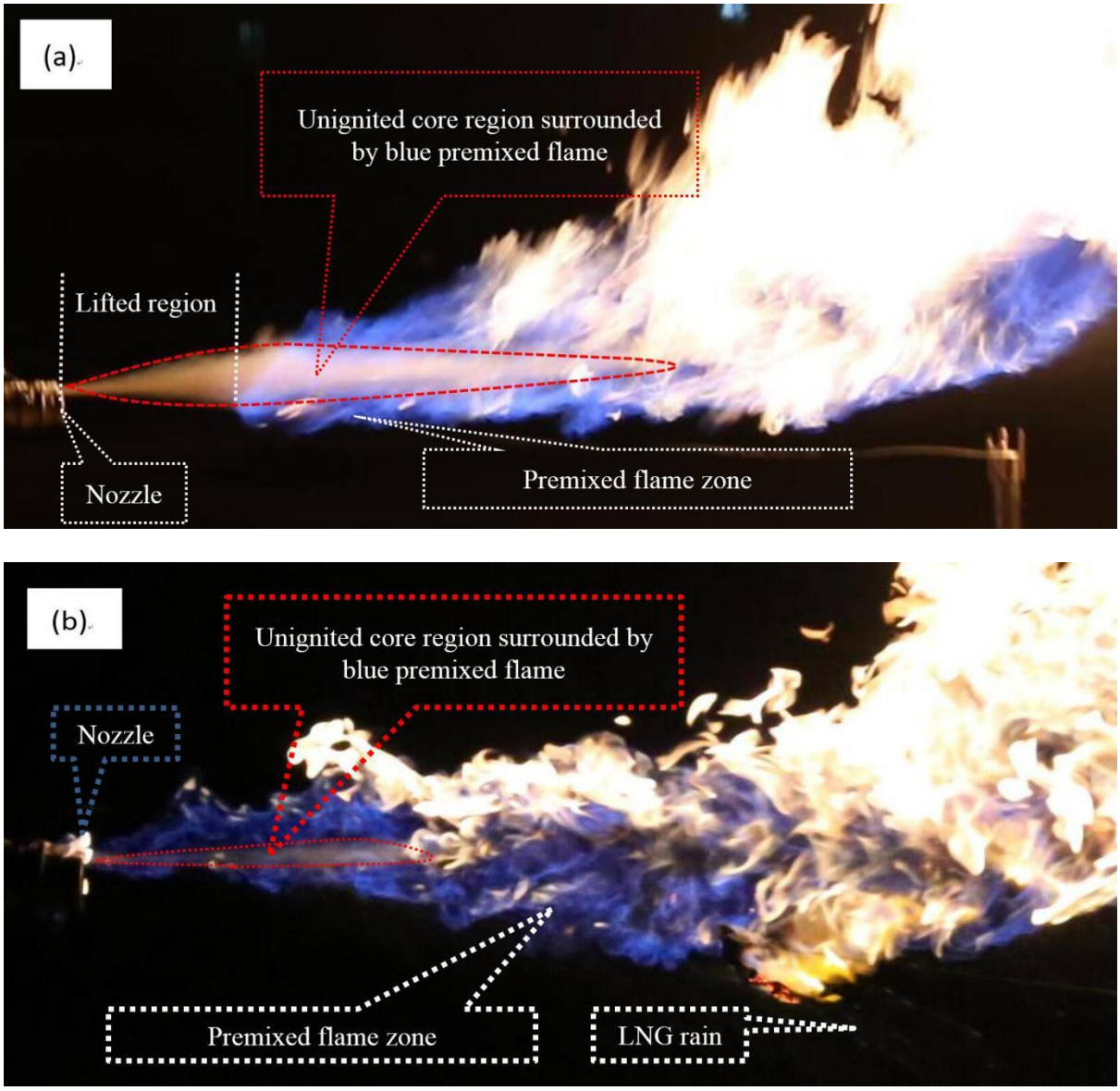

Fig. 4. The resulting LNG jet fire near the nozzle: (a) LNG flow rate 0.04kg/s; (b) LNG flow rate 0.02kg/s.

The LNG vapour was difficult to ignite close to the nozzle. In the tests, the jet was ignited 2 m from the nozzle as shown in Figs. 1 and 2. Following the ignition, the resulting jet fire quickly propagated towards downstream as well as backwards towards the nozzle. Eventually a stable LNG jet fire formed. Figure 3 shows the resulting jet fires from the release rates of 0.04 and 0.02 kg/s with the nozzle diameter d = 10mm. When the rate of LNG injection increased from 0.02 to 0.04kg/s, the horizontal flame extent changed from 3.5 to 5m. Here the horizontal flame extent refers to the horizontal distance from the nozzle outlet to the flame tip.

For clarity, Figure 4 is zoomed in on the region near the nozzle. The jet flame, from the release rate of 0.04 kg/s under the injection pressure of 8.5 bar, was lifted from the nozzle. There was no combustion in the core region which consisted of unburnt LNG jets surrounded by blue premixed flame, which was caused by the slow evaporation rate of the LNG and well

mixing with the surrounding air. Gradually, the outer region contained both premixed and diffusion flames. Pockets of premixed blue flames can be seen further downstream in the outer edge of the intermittent jet flame from the end of this no-combustion core region.

In the case of the release rate of 0.02 kg/s under the injection pressure of 5.5 bar, the flame spread backwards to the nozzle and stabilised there as shown in Figs. 3 and 4 (b). There still existed a non-combusting core but its size was much smaller than the previous case with release rate of 0.04 kg/s under the injection pressure of 8.5 bar. This unburnt LNG core was also surrounded by blue premixed flame in the outer region. More regions of premixed blue flames were also observed further downstream of the jet fire. The existence of these additional premixed flame regions was thought to be caused by the relatively slow initial propagation of the flame and further evaporation of the LNG which were carried downstream, resulting in pockets of premixed regions which were later ignited.

The rainout of the LNG jet was observed in the case of the release rate of 0.02 kg/s under the injection pressure of 5.5 bar, forming an LNG pool on the ground. The LNG pool continued to absorb heat from the surroundings including the jet fire and evaporate. In the tests, the evaporating LNG pool was manually ignited, resulting in an LNG pool fire as shown in Fig.5.

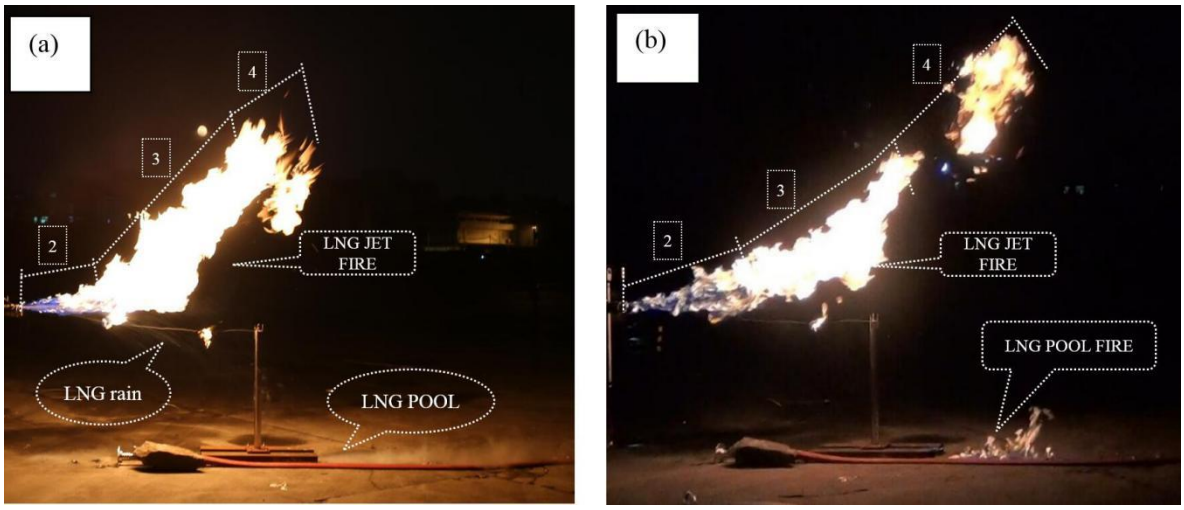

Fig.5. LNG jet fire and pool fire.

3.2 Flame shape

Most previous research has utilized the "visible flame" extracted from visualizations (Mogi and Horiguchi, 2009; Kalghatgi, 1983) to represent the flame shape. But as pointed out by Palacios and Casal (2011), it is hard to apply the concept of visible flame since the flame might become totally transparent with enhanced combustion resulting from increasing mixing of air and fuel. The temperature contours from IR images have also been used to define the flame boundary by Palacios and Casal (2011) and Upatnieks et al. (2004). Cumber and Spearpoint (2006) determined the visible flame boundary as equating to a heat flux of 40 W/m^2 while some others have regarded temperature contours as 600K or 800K (Palacios and Casal,

2011; Upatnieks et al., 2004).

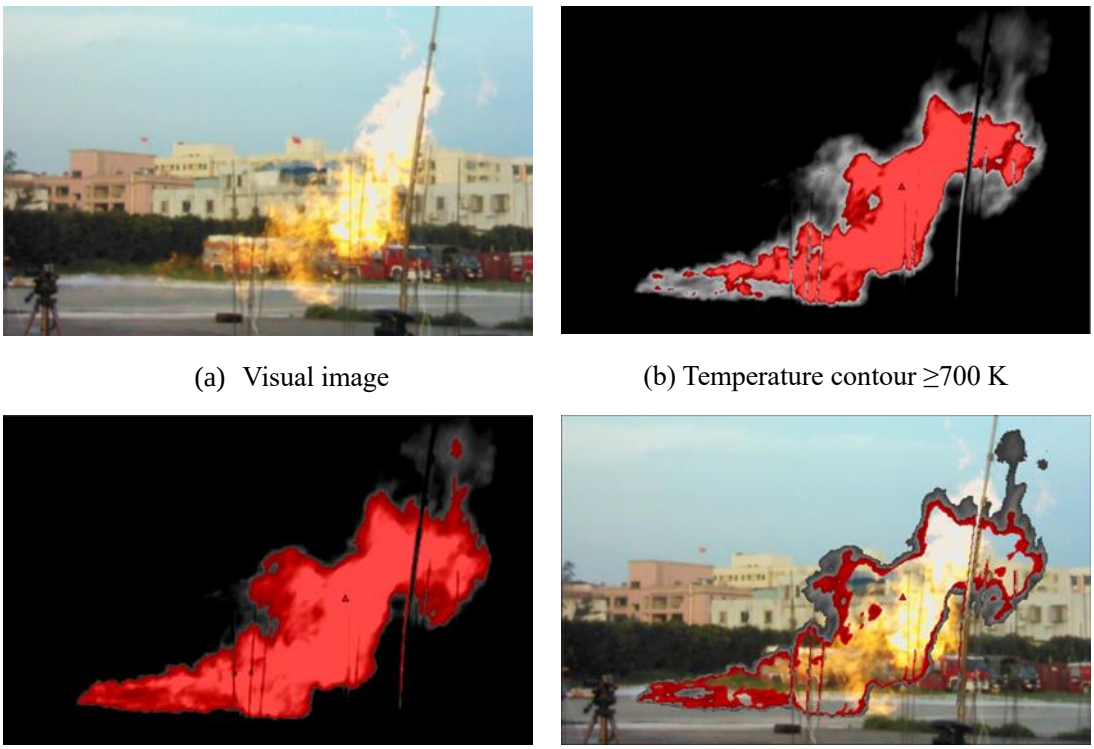

(a) Visual image

(b) Temperature contour ≥700 K

(c) Temperature contour ≥500 K

(d) The flame with a 600K temperature contour

Fig.6. An infrared image employing the isotherm of 600 K to match with visual image.

In the present study, both CCD and IR camera were employed to capture the shape of flame by taking several images for comparison. A regular visible photo and an infrared image recorded by the IR camera FLIR T660 each time are comprised of a matrix of 640 by 480 pixels. Each pixel's value corresponds to the black body temperature recorded by the IR camera. A temperature of 600K was singled out after several varied temperatures were tested to define the flame boundary.

At a temperature ≥500K, the area occupied by the flame in the IR image was found to be larger than the image of the visible flame shown in Fig. 6. However, when the temperature was greater than or equal to 700k, the area occupied by the jet flame was smaller than that occupied by the visible image. As for the temperature ≥600 K, the visible and infrared jet flame images overlapped in good agreement. Therefore, the 600 K isotherm was used to define the flame boundary.

The Matlab Image Processing Toolbox was used to process the IR images so that the flame boundary corresponding to a certain black body temperature could be set apart. From a given contour, the flame length was identified as the maximum horizontal pixel value of the contour, and the flame elevation (H_f) was defined as the maximum elevation about the ground.

Previous experimental studies (Gopalaswami et al., 2016; Mogi et al., 2011) of small-

scale methane, LPG (Liquefied Petroleum Gas) and liquefied DME (dimethyl ether) flames suggested that the shape of horizontal jet fires can be approximated by rectangular, kite or ellipse shape. However, the images in Figs. 6 and 7 show that the LNG jet fires gradually tilted upwards. In comparison with other liquid fuels, the cryogenic LNG evaporated more quickly following the release due to the relatively large differences of the surrounding temperature and the LNG boiling point. The heat exchange with the surrounding air also resulted in the increase of the temperature of the LNG vapour, enabling it to rise gradually. Eventually the density of the LNG vapour became lower than the air.

The whole LNG jet flame can be regarded as an upward curved axisymmetric cone. The curved path of the flame axis is considered a good representation of the LNG jet flame shape. Figure 8 is plotted by selecting points along the flame axis in Fig. 7. It illustrates that the horizontal LNG jet fire extended both horizontally and upwards.

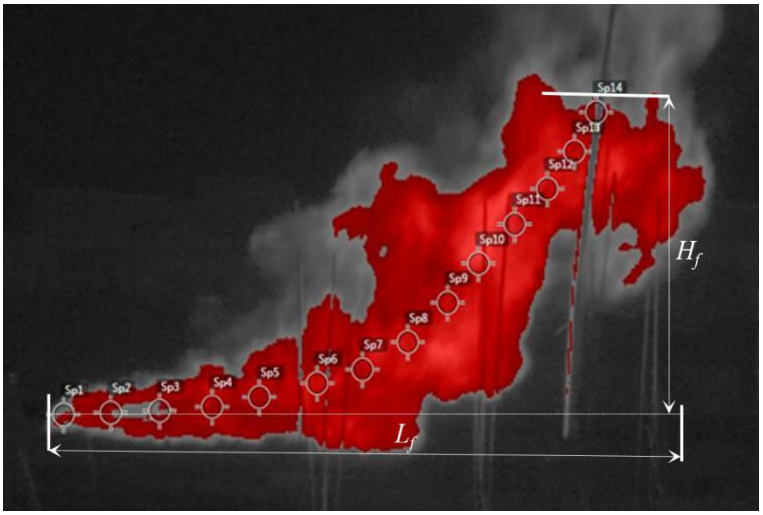

Fig.7. Flame shape based on IR contour.

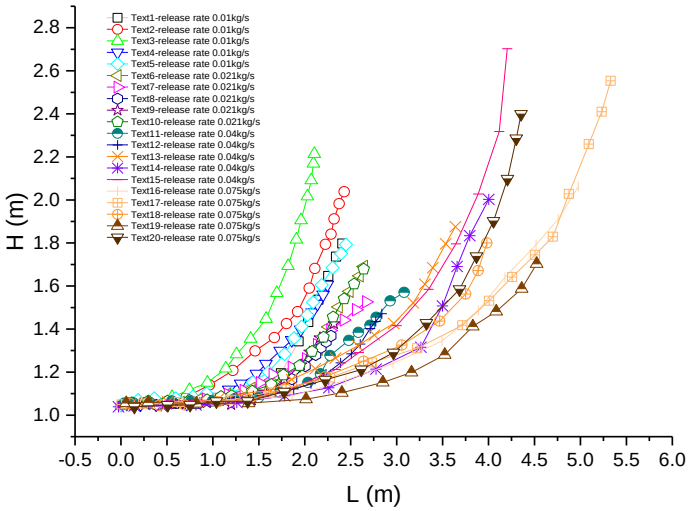

Fig.8. Flame centreline based on the IR contour.

3.3 Flame temperature

Figure 9 presents four images of the four fluxes taken with the IR video cameras. The length of the fire, the rising height and the maximum temperature all changed with the LNG release rate.

Figures 5 and 9 show that the flame temperature in the premixed flame zone is relatively low. As observed in the experiments, there was a core region of LNG near the nozzle which did not evaporate. The premixed flame region was hence fuel lean, resulting in much lower temperature than the rest of the jet fire. For example, at an equivalence ratio of 0.15, the adiabatic flame temperature is approximately only 700 K.

Figure 10 plots the peak temperatures from 30 ~160 s. The average peak temperatures were 1366 K, 1341 K, 1244 K and 1033 K for the LNG release rates of 0.075, 0.06, 0.04 and 0.02 kg/s respectively. These temperatures were calculated with the camera emissivity set to 0.5.

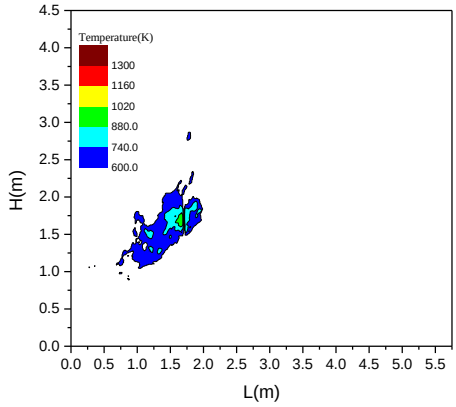

（a）0.01kg/s

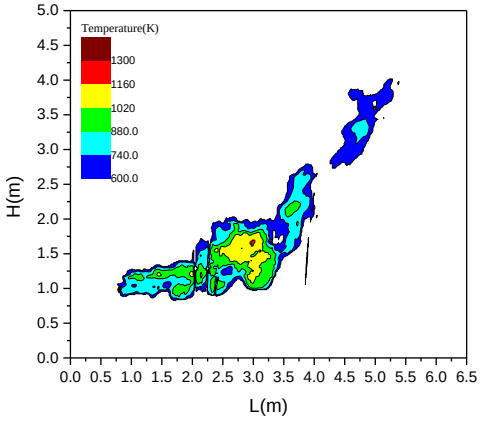

(b) 0.021kg/s

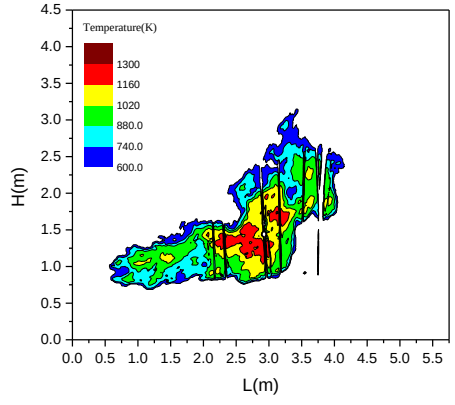

(c) 0.04 kg/s

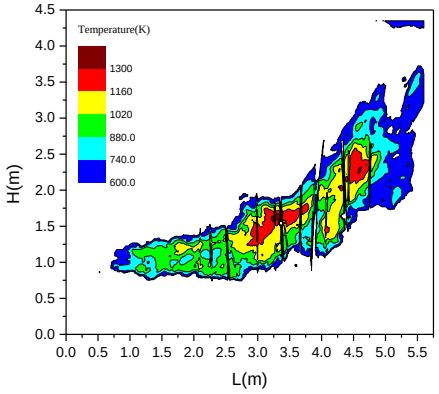

(d) 0.075 kg/s

Fig.9. IR camera images in Test 1-4.

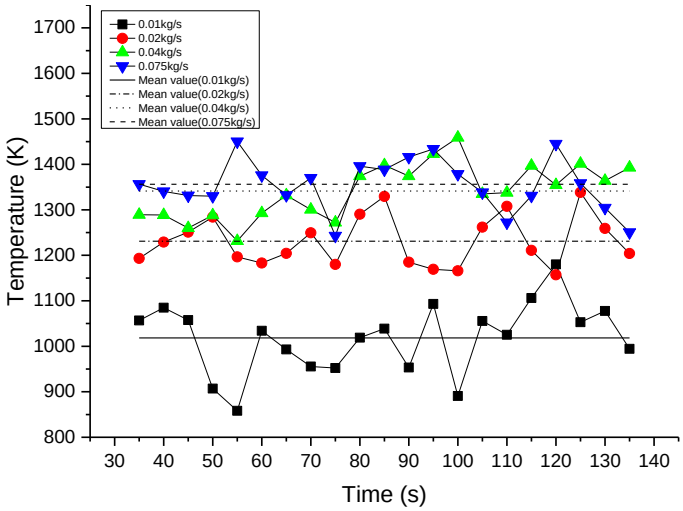

Fig.10. The peak temperatures in Tests 1-4.

3.4 Flame length

There are various definitions of the flame length in the literature. Most previous researchers defined the flame length as the distance from the nozzle to the furthest point on the flame envelope, and the flame lift-off distance denotes the distance from the nozzle to the closest point on the lower edge of the flame envelope. Lowesmith and Hankinson (2013) calculated the flame length and lift-off length after the jet reached quasi-steady state. Smith et al. (2005) and Palacios et al. (2009) determined the flame length from the measurements of the flame images recorded by CCD and high-speed cameras and took the average values. More recently, some investigators calculated the flame length from IR images (Lowesmith and Hankinson, 2012; Palacios and Casal, 2011; Simpson et al.). The number of images used in the flame length calculation was not always specified and could be varied ranging from 30 to 90 images or a time interval of 10s (Lowesmith and Hankinson, 2012; Røkke et al., 1994).

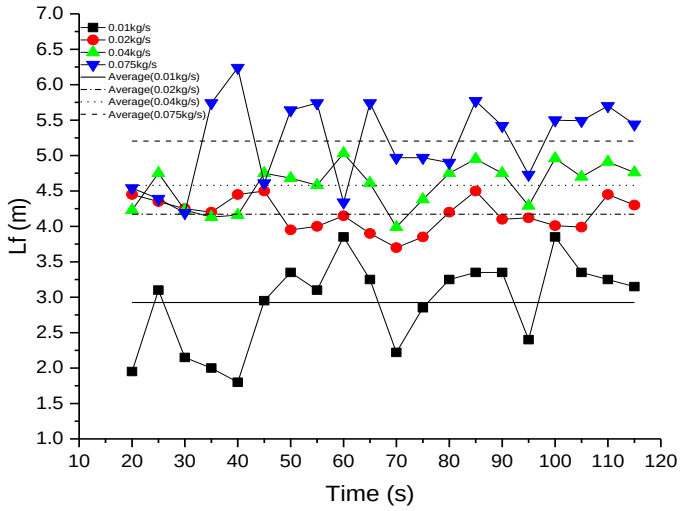

Fig.11. Time variations of the values of the flame length.

Zhang et al. (2017) obtained flame intermittency distribution by averaging the values of consecutive binary images converted from time series of flame videos. In the present study, the IR images were used for calculating the flame length as it was difficult to record the LNG flame by CCD camera during daylight.

The infrared camera took IR images every 5 seconds during steady combustion, and a total of 20 IR images were chosen to calculate the flame length for each experiment. Each infrared picture was firstly converted to temperature field by colorimetric method, and then the greatest horizontal distance (L_f) of 600K was obtained.

As the experiment was carried out outdoors, the ambient wind (0-0.05m/s) affected the flame stability greatly, which led to the fluctuation of the flame length measurements. For this reason, the mean value from the 20 measurements was taken as the flame length value for each experiment.

Figure 11 shows the time variations of the flame length. The mean flame length is 5.2 m, 4.58 m, 4.17 m and 2.93 m for the LNG release rates of 0.075, 0.06, 0.04 and 0.02 kg/s respectively. Apparently, the flame length increases with the increase of the LNG release. In Fig. 12, the average flame length is plotted against the LNG release rate. The results correlate well with the following formula modified from that of Mogi et al. (2011) and FABIG technical note (2010):

$$L_f = 10.1 * m_l^{0.248} \tag{1}$$

The flame length L_f is proportional to the 0.248 power of the mass flow rate m_l in the case of the nozzle diameter of 0.01m. In comparison with other liquid fuels, LNG jets vaporise much more quickly upon releasing into the atmosphere. Mogi et al. (2011) and FABIG (2010) suggested similar correlations for the flame length of liquefied DME jet fire. The results here suggest that the combustion characteristics of the flashing LNG are like spray combustion.

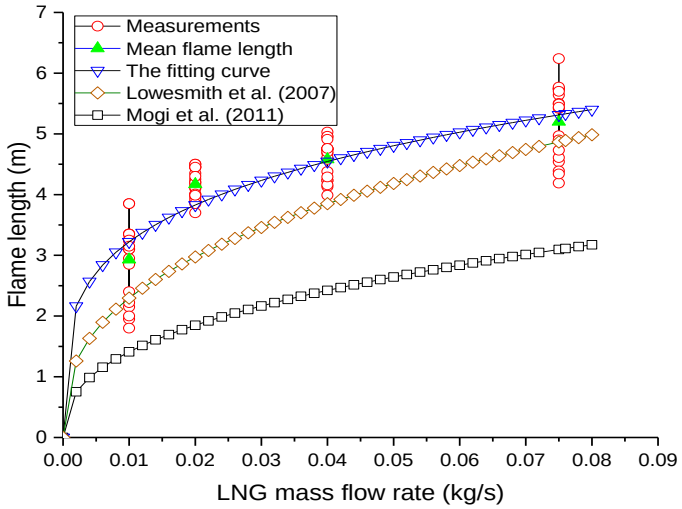

Fig.12. Relation between the flame length and the mass flow rate.

3.5 Flame radiation

The incident radiative heat fluxes were measured by five radiometers as shown in Fig.13, thus the thermal hazards from the fire could be investigated. The locations of each radiometer in the tests are summarized in Table 4 with the coordinated origin shown in Fig. 13. As expected, within each jet flame, the radiative heat fluxes decrease with the increase of the distance from the nozzle and the incident radiative heat fluxes increase with the increase of the LNG release rate.

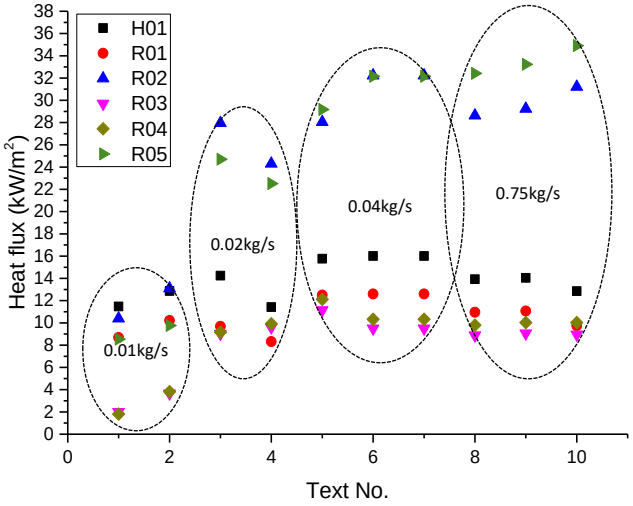

Fig.13. The incident radiative heat fluxes at various locations in 10 tests.

Table 4. Radiometer Position in Tests

Radiometer No.	x[m]	y[m]	z[m]
H01	0	0	1.5
R01	0	0	1.5
R02	2.3	3.1	1.5
R03	2.3	4.5	1.5
R04	4.6	3.1	1.5
R05	4.6	4.5	1.5

R02 and R05 were placed at a similar distance (y-value) from the flame, but R02 had a larger radiation than R05 at a higher flow rate (0.75kg/s), because its flame length increased with the acceleration of the average LNG jet velocity, whereas R05 was closer to the centre of the flame along the flame axis (x-value). Even though R02 @ R03 and R04 @ R05 were placed at a similar distance in x-value, the data changes of R03 and R04 are not remarkable like those of R02 and R05. Through data comparisons, with the LNG jet rate increasing, the increasing trend of jet flame length become more evident comparing that in the fire diameter.

Heat flux meter (H01) and R01 were placed 25cm over the nozzle, and the measurements

suggest that the heat flux and radiant heat flux density are lower than R02 and R05 despite their proximity to the jet nozzle.

4. Conclusions

Full-scale field tests were conducted using horizontally oriented nozzle for flashing LNG jet fires. The flame characteristics, shape, length, temperature, radiation hazards were measured in different release conditions. The main findings can be summarized as follows:

(1) LNG jet fire can be divided into four zones. In order from bottom to top, the lifted region, the premixed flame region (blue region), the anchored pulsating region and the intermittency region which stretches out along the central line. In some cases, part of the LNG did not vaporize in the flame zone but rained out onto the ground to form an LNG pool, the ignition of which resulted in an LNG pool fire.

(2) The horizontal LNG jet fire tilted upwards. This trend differs from that of horizontal LPG jet fires.

(3) With the increase of the flow rate from 0.01kg/s to 0.075kg/s, the peak temperature of the LNG jet fire also increased and stabilized at about 1100℃.

(4) A new correlation, in similar format as previously used for liquefied DME jet fire, was found to correlate well the measured flame length with mass flow rate: $L_f = 10.1 * m_l^{0.248}$

(5) For different release rates, the incident radiative heat fluxes remained at almost the same level in regions close to the release point. However, they increased with the increase of the LNG release rate, though further away from the release point.

Acknowledgments

This work is supported by Guangdong Provincial Key Laboratory of Fire Science and Technology (No. 2010A060801010). Dr Vendra C. Madhav Rao of University of Warwick is acknowledged for helpful discussion.

References:

Cleaver P, Johnson M, Ho B, 2007. A summary of some experimental data on LNG safety. J. Hazard. Mater. 140(3): 429-438. https://doi.org/10.1016/j.jhazmat.2006.10.047.

Cumber PS, Spearpoint M, 2006. A computational flame length methodology for propane jet fires. Fire Safety J. 41(3): 215-228. https://doi.org/10.1016/j.firesaf.2006.01.003.

Gopalaswami N, Liu Y, Laboureur DM, Zhang B, Mannan MS, 2016. Experimental study on propane jet fire hazards: Comparison of main geometrical features with empirical models. J. Loss Prevent. Proc.

41(Supplement C): 365-375. https://doi.org/10.1016/j.jlp.2016.02.003.

FABIG Technical Note 11, 2010. Fire Loading and Structural Response.

Havens J, 1992. Review of dense gas dispersion field experiments. J. Loss Prevent. Proc. 5(1): 28-41. https://doi.org/10.1016/0950-4230(92)80062-D.

Kalghatgi GT, 1983. The visible shape and size of a turbulent hydrocarbon jet diffusion flame in a cross-wind. Combust. Flame 52(Supplement C): 91-106. https://doi.org/10.1016/0010-2180(83)90123-2.

Koopman RP, Cederwall RT, Ermak DL, Goldwire HC, Hogan WJ, McClure JW, McRae TG, Morgan DL, Rodean HC, Shinn JH, 1982. Analysis of Burro series 40-m3 lng spill experiments. J. Hazard. Mater. 6(1): 43-83. https://doi.org/10.1016/0304-3894(82)80034-4.

Lowesmith BJ, Hankinson G, 2013. Large scale experiments to study fires following the rupture of high pressure pipelines conveying natural gas and natural gas/hydrogen mixtures. Process Saf. Environ. 91(1): 101-111. https://doi.org/10.1016/j.psep.2012.03.004.

Lowesmith BJ, Hankinson G, 2012. Large scale high pressure jet fires involving natural gas and natural gas/hydrogen mixtures. Process Saf. Environ. 90(2): 108-120. https://doi.org/10.1016/j.psep.2011.08.009.

Lowesmith BJ, Hankinson G, Acton MR, Chamberlain G, 2007. An Overview of the Nature of Hydrocarbon Jet Fire Hazards in the Oil and Gas Industry and a Simplified Approach to Assessing the Hazards. Process Saf. Environ. 85(3): 207-220. https://doi.org/10.1205/psep06038.

Luketa A, Blanchat T, 2015. The phoenix series large-scale methane gas burner experiments and liquid methane pool fires experiments on water. Combust. Flame 162(12): 4497-4513. https://doi.org/10.1016/j.combustflame.2015.08.025.

Luketa-Hanlin A, 2006. A review of large-scale LNG spills: Experiments and modeling. J. Hazard. Mater. 132(2): 119-140. https://doi.org/10.1016/j.jhazmat.2005.10.008.

Mogi T, Horiguchi S, 2009. Experimental study on the hazards of high-pressure hydrogen jet diffusion flames. J. Loss Prevent. Proc. 22(1): 45-51. https://doi.org/10.1016/j.jlp.2008.08.006.

Mogi T, Shiina H, Wada Y, Dobashi R, 2011. Experimental study on the hazards of the jet diffusion flame of liquefied dimethyl ether. Fuel 90(7): 2508-2513. https://doi.org/10.1016/j.fuel.2011.03.026.

Palacios A, Casal J, 2011. Assessment of the shape of vertical jet fires. Fuel 90(2): 824-833. https://doi.org/10.1016/j.fuel.2010.09.048.

Palacios A, Muñoz M, Casal J, 2008. Jet fires: An experimental study of the main geometrical features of the flame in subsonic and sonic regimes. Aiche J. 55(1): 256-263. https://doi.org/10.1002/aic.11653.

Puttock JS, Blackmore DR, Colenbrander GW, 1982. Field experiments on dense gas dispersion. J. Hazard. Mater. 6(1): 13-41. https://doi.org/10.1016/0304-3894(82)80033-2.

Raj PK, 2007. LNG fires: A review of experimental results, models and hazard prediction challenges. J. Hazard. Mater. 140(3): 444-464. https://doi.org/10.1016/j.jhazmat.2006.10.029.

Røkke NA, Hustad JE, Sønju OK, 1994. A study of partially premixed unconfined propane flames. Combust. Flame 97(1): 88-106. https://doi.org/10.1016/0010-2180(94)90118-X.

Simpson RB, Jensen RP, Demosthenous B, Luketa AJ, Ricks AJ. The Phoenix series large scale LNG pool fire experiments..

Smith T, Periasamy C, Baird B, Gollahalli SR, 2005. Trajectory and Characteristics of Buoyancy and Momentum Dominated Horizontal Jet Flames From Circular and Elliptic Burners. Journal of Energy Resources Technology 128(4): 300-310. http://dx.doi.org/10.1115/1.2358145.

Upatnieks A, Driscoll JF, Rasmussen CC, Ceccio SL, 2004. Liftoff of turbulent jet flames—assessment of edge flame and other concepts using cinema-PIV. Combust. Flame 138(3): 259-272. https://doi.org/10.1016/j.combustflame.2004.04.011.

Zhang X, Hu L, Zhang X, Tang F, Jiang Y, Lin Y, 2017. Flame projection distance of horizontally oriented buoyant turbulent rectangular jet fires. Combust. Flame 176(Supplement C): 370-376. https://doi.org/10.1016/j.combustflame.2016.10.016.